DTIC FILE COPY (12)

ERL-0396-TR

AR-004-885

AD-A186 106

AUSTRALIA

# DEPARTMENT OF DEFENCE

## DEFENCE SCIENCE AND TECHNOLOGY ORGANISATION

## ELECTRONICS RESEARCH LABORATORY

DEFENCE RESEARCH CENTRE SALISBURY
SOUTH AUSTRALIA

TECHNICAL REPORT

ERL-0396-TR

# A MATHEMATICAL MODEL FOR SIMULATING INFRARED IMAGES OF SHIPS

O.S. SCOTT

DTIC
ELECTE
OCT 1 6 1987
S D
D

"Original contains color plates: All DTIC reproductions will be in black and white"

DISTRIBUTION STATEMENT A
Approved for public release;
Distribution Unlimited

Approved for Public Release

COPY No. 31

© Commonwealth of Australia

DECEMBER 1986

The official documents produced by the Laboratories of the Defence Research Centre Salisbury are issued in one of five categories: Reports, Technical Reports, Technical Memoranda, Manuals and Specifications. The purpose of the latter two categories is self-evident, with the other three categories being used for the following purposes:

| | | |
|---|---|---|
| Reports | : | documents prepared for managerial purposes. |
| Technical Reports | : | records of scientific and technical work of a permanent value intended for other scientists and technologists working in the field. |
| Technical Memoranda | : | intended primarily for disseminating information within the DSTO. They are usually tentative in nature and reflect the personal views of the author. |

UNCLASSIFIED

AR-004-885

DEPARTMENT OF DEFENCE

DEFENCE SCIENCE AND TECHNOLOGY ORGANISATION

ELECTRONICS RESEARCH LABORATORY

TECHNICAL REPORT

ERL-0396-TR

# A MATHEMATICAL MODEL FOR SIMULATING INFRARED IMAGES OF SHIPS

O.S. Scott

## S U M M A R Y

This element-contribution model is programmed so that the distribution of infrared radiation from a ship target can be calculated for any aspect and any infrared waveband. The present application is to simulate the images formed by the guidance system of an imaging infrared antiship missile.

The input data needed are the surface temperatures and emissivities and shapes of the main structures and the equivalent black body temperatures of the sky and sea surface. The shape of each ship is represented as a number of 'boxes' with each side and the top of each box represented by faces of elementary cubes. The positions and the centres of each face are calculated from the positions of three rows of elementary faces measured from plans for each box.

The output is an array of numbers representing the radiant intensity from the unscreened faces in the required direction and for the defined waveband. This array can be converted to a colour-coded image on a video display for testing and presentation purposes.

POSTAL ADDRESS: Director, Electronics Research Laboratory,
Box 2151, GPO, Adelaide, South Australia, 5001.

UNCLASSIFIED

TABLE OF CONTENTS



LIST OF FIGURES



Accession For
NTIS CRA&I
DTIC TAB
Unannounced
Justification
By
Distribution/
Availability Codes
Dist Avail and/or Special
A-1

DTIC COPY INSPECTED 6

Page

LIST OF APPENDICES

# 1. INTRODUCTION

Ships may be attacked by sea-skimming missiles and guided bombs which have infrared guidance systems. Infrared and Optical Countermeasures Group at Electronics Research Laboratory has been tasked by the Royal Australian Navy to investigate the vulnerability of ships to infrared weapons, and to study the effectiveness of possible countermeasures such as signature reduction and the use of decoys. Guidance systems of the imaging type are likely to be especially difficult to counter by decoys, because the spatial distribution of radiation from the target in the guidance system waveband must be approximated by the decoy. Good representations of the spatial distribution of radiation from targets are therefore needed for countermeasures studies.

This report describes a target model for use with simulations of imaging infrared systems with specified wavebands which may be used together with a missile model and an atmospheric attenuation model to study the effectiveness of infrared countermeasures.

The target model is outlined in Section 2, and described in detail in Section 3. Samples of the displayed output are given in figure 1.

# 2. OUTLINE OF METHOD

The objective of the simulation is to provide the distribution of target radiant intensity presented perpendicular to the sight line from the missile. This is achieved by considering small elements of the ship surfaces in turn, and calculating their positions and whether or not they are visible from the missile. If they are not screened by other elements the positions of their projections on a plane perpendicular to the sight line from the missile (the 'output' plane) are calculated, and small areas centred on these projections are recorded as parts of the projected image. At the same time these areas are assigned the temperatures, emissivities and inclinations to the vertical associated with the elements concerned, which are those assigned to the surfaces of the major structures of the ship.

The shape of the ship is defined in terms of a small number of boxes, with each face of each box considered as made up of a large number of elementary faces. These elementary faces are the visible faces of the large number of elementary cubes representing the box shape. The calculations for the projections are based on the element positions relative to ship axes, and the positions of the missile and ship and the heading of the ship in reference axes (figure 2).

As a simple example, figure 3 represents a target considered as one box only. The shape data are the x coordinates of the centres of the squares in the top row and bottom row of the starboard side; and the y coordinates of the centres of the squares in the starboard side row of the top face, all measured from the first x position at the stern to the last at the bow. These three sets of data are used as described in Section 3.2 to define the positions of every elemental face in each face of the box.

The temperature, emissivity and inclination data are the separate values assigned for the whole of the top, port side, starboard side, stern and bow. If as shown the box comes to a point at the bow, there is no bow face. The values of temperature may be nominal values or values calculated as described in Section 3.3. A nominal 'ship centre' is also defined in the ship axis system. The decks are assumed to be horizontal, and the sides vertical unless otherwise defined.

There can be several different elements corresponding to any given point on the output plane. A calculation of range to the missile is carried out for each element to ensure that the one closest to the missile is used to define the surface temperature for each output plane point.

The array of temperatures corresponding to elements of the output plane is converted to an array of radiant intensities by using:

(a) the presented area represented by each element;

(b) the temperature and emissivity of each element;

(c) the appropriate gray-body distributions convolved with the required spectral responses; and

(d) the inclination of each element, and sky and sea surface equivalent black body temperatures which are required for the calculation of ship surface radiances.

A spectral distribution of the radiant intensity is retained for each value of temperature used so that the results may be further convolved with an atmospheric transmission model and any other seeker waveband when required.

The results may be presented as an array of surface temperatures or radiant intensities, or as a colour-coded image.

## 3. DESCRIPTION OF MODEL

### 3.1 Input required

The input section is the first part of the flow diagram of the model shown in figure 4. After initialising the variables, the program prompts the user to supply details of the engagement to be simulated. It is necessary to supply the position and heading of the ship, and the missile position, all with respect to a set of reference axes; and to define the particular ship which is to be simulated and the type of output display required. At this stage it is possible to limit the calculations to one of two infrared wavebands (3 to 5 μm or 8 to 14 μm).

The data defining the shape and temperatures of the designated vessel are then read from the appropriate file, which defines the small number of "boxes" used to represent the shape, and the three arrays of coordinates defining the starboard face of each box as described in figure 3. It also includes the temperatures emissivities and inclinations to be assigned to each face of each box.

The temperatures used are derived from values measured in overcast conditions. Temperature increases caused by solar heating may be incorporated by incrementing these temperatures as described in Section 3.3.

### 3.2 Calculations

#### 3.2.1 Face perimeters

The positions of all the elements forming boundaries of faces for each box are calculated by reflection and manipulation of the input data read from file.

The positions of the elements in the perimeter of the port face of each box are obtained from a simple reflection of the input starboard face data in the x-z plane which is the plane of symmetry of the ship.

The perimeter of the top face of each box is obtained from the input data for the top of the starboard face together with the same data reflected in the x-z plane.

The stern face is considered to be vertical with boundaries defined by the positions of the rear upper and lower corners of the starboard and port faces. If the stern upper elements of the port and starboard sides are adjacent, there is no stern face.

The perimeter of the front face is similarly defined from the positions of the bow upper and lower elements of the port and starboard faces.

3.2.2 Calculation of computing loop limits

The computations on the surface elements to determine their projected positions on the output plane, and their radiance values are carried out in "nested" iterations. The outer nest covers the box number, and the next the face number (eg Starboard-1, Port-2, Top-3, Stern-4, Bow-5). The next nest covers the sections along the ship axis (the x coordinate changes) from the stern to the bow. The final loop is either:

(a) over the range of values of height (z) at constant distance from the x-z plane (y) for the vertical sides; or

(b) over the range of values of y from one side to the other of the flat top at constant z; or

(c) over the range of values of both y and z for the stern and bow.

It should be noted that the cross sections of all faces perpendicular to the x axis are represented as either vertical or horizontal lines. This limitation does not affect the appearance of the images to any noticeable degree. However the inclinations of the faces to the vertical are taken into account for calculating the contributions of reflection from sky and sea surface to total radiant intensities (see Appendix II).

3.2.3 Element mapping

The rotation constants, which depend on the heading of the ship and its position relative to the missile, and which are independent of position on the ship, are calculated in a subroutine outside the iteration loops in which the mapping of element positions onto the output plane are performed.

The mapping is carried out by converting the x,y,z coordinates of individual elements into three coordinates ($x_p$, $y_p$, $z_p$) in a system where $X_p$ is the direction from observer to ship, $Y_p$ has the direction of $v \times X_p$ where v is the upward vertical, and $Z_p$ completes the right handed orthogonal set. $Z_p$ $Y_p$ is the output plane and $y_p$, $z_p$ the coordinates of the projected point in this plane. The equation for this conversion is:

$$\begin{pmatrix} x_p \\ y_p \\ z_p \end{pmatrix} = A_2(\Theta)\ A_1(\psi) \begin{pmatrix} x \\ y \\ z \end{pmatrix} \qquad (1)$$

where $A_1$, $A_2$ are the familiar rotation matrices (see Appendix I) and $\psi$ and $\theta$ are rotations which are derived in Appendix I.

As each element is mapped onto the output plane, $x_p$ provides a measure of the range from the element to the missile. The temperature assigned to each position in the output plane is that associated with the element closest to the missile which has been mapped onto that position. By this means the masking of any part of the ship by any other part is incorporated in the model.

Owing to rounding errors in the computations it was found that small sections of the rotated image were blank or showed sections which should have been masked. This was overcome by assigning the temperature of any element of the output plane to the next in increasing value of $y_p$ and $z_p$ (and a fourth element to complete the square). These additional elements were normally overwritten by subsequent mapping, but the effect was to fill in the minor gaps. A further effect of this technique was to increase the size of each mapped face by one element in the $y_p$ direction and one element in the $z_p$ direction. If the element size is small compared with the face size this effect is of no consequence. The effect can however be eliminated by reducing the input data values by one unit in each direction.

### 3.2.4 Calculation of radiated and reflected radiant intensities

The radiant intensity of each element of the output plane array depends on the presented area A it represents (which is the same for all elements in the output plane), the temperature (T°K) and emissivity ($\varepsilon$) of the ship element it represents, and the infrared waveband chosen. The radiant intensities (W/sr) are calculated using the Planck formula:

$$H_{\lambda_1-\lambda_2} = \frac{\varepsilon A}{\pi} \int_{\lambda_1}^{\lambda_2} \frac{C_1\ \lambda^{-5}\ B_\lambda\ d\lambda}{\exp(C_2/\lambda T)-1} \qquad (2)$$

where $C_1$ and $C_2$ are the first and second radiation constants $3.74 \times 10^{-12}$ W cm², and 1.438 cm°K respectively, $\lambda$ is wavelength in centimetres, and $B_\lambda$ is the normalised spectral sensitivity characteristic of the sensor from wavelength $\lambda_1$ to $\lambda_2$.

In addition to the energy radiated from the surface, a proportion of the energy originating in the hemisphere it subtends is reflected. The additional radiant intensity from this source is given by:

$$J_{REF\lambda_1-\lambda_2} = \frac{A\ (1 - \varepsilon)\ E_T}{\pi}$$

An expression for $E_T$, the energy received from the background by the element, is derived in Appendix II. The case considered is for a uniform sea background, a sky background radiance which is a function of elevation angle only, and a perfectly diffuse surface of the element A.

In order to calculate the irradiance at the missile from each element it is also necessary to incorporate the atmospheric transmission ($t_\lambda$) in the integration of equation (3). At present this is performed by using Lowtran(ref.1).

Since there are in general only about ten boxes each with five faces, there are only about fifty temperatures to consider. The radiant intensity and irradiance calculations are performed outside the iteration loops and only once for each value of temperature assigned in the model to avoid repeating the calculations for each element.

### 3.3 Output presentation

The output may be presented as a printed array of the values of surface temperature, radiant intensity, or irradiance; or as an array of symbols with a key for conversion to the necessary values.

A black and white shaded image can be used to represent the spatial distribution of temperature, radiant intensity or irradiance with an appropriate key, and colour can be used instead of or as well as shading.

The type of presentation required is selected by the user at the start of the simulation.

## 4. PRESENT APPLICATION OF THE MODEL

The target model is intended to be part of a simulation of missile attacks on ships, during which infrared countermeasures may be used. So far the geometry of an FFG Frigate (HMAS Canberra), a Destroyer Escort (HMAS Torrens) and a Guided Missile Destroyer (HMAS Perth), and a Coastal Minesweeper (MHI) have been modelled. Surface temperatures have been derived from trials in which thermovision cameras recorded the infrared images of some of these ships.

The background is represented as a constant irradiance from the sea surface, and an irradiance equivalent to that from a black body at ambient temperature (with no atmospheric attenuation) for the horizon sky. The irradiance from the sky reduces to zero linearly with elevation angle up to 90°. This representation requires refinement for representations of specific environments. The position of the waterline on the ship relative to the horizon is calculated from the height of the missile, the range of the ship, and the radius of the earth (Appendix III).

## 5. MODEL DEVELOPMENT

### 5.1 Irradiance from exhaust plumes

For missiles using the infrared waveband which covers the carbon dioxide emissions near 4.4 μm, the engine exhaust plumes can be significant sources. This is particularly so for the FFG vessels which have gas turbine engines.

A series of trials were carried out for various purposes on an FFG in March 1983(ref.2). The video records of plume signatures are being analysed in an attempt to derive empirical models of:

(a) irradiance from the plumes as a function of range, aspect, and engine condition; and

(b) plume shape as a function of wind speed and direction, ship speed and direction, aspect, and engine condition.

During the same trials period limited measurements were also made on a destroyer escort with a steam turbine.

Examples of 8 to 14 and 3 to 5 μm images of HMAS Canberra are shown in figure 5. The plume is the dominant feature of the 3 to 5 μm signature of the FFG at the range of the measurement. The images shown were produced with the analysis system described in reference 3.

It is hoped that it will be possible to incorporate a three-dimensional representation of FFG and DE plumes in the target model following analysis of trials data.

### 5.2 Background representation

(1) Sea background

The radiance of the sea surface is partly grey-body radiation at the sea temperature and partly reflection of the sky. Since sky radiance is in general a function of elevation angle, the sea radiance will be a function of the declination of the sight line. Sea roughness may be considered as the variation of slope of areas of surface with certain spatial and temporal correlation characteristics. Variation of surface angle will produce variations of the reflected component of sea radiance. To produce a target model which incorporates sea clutter, the surface shape variations must be modelled so that the spatial and temporal changes are derived as functions of local wind speed and direction (and possibly other parameters affecting sea surface shape). Such models do exist, for example(ref.2,3), and considerable work has been carried out to estimate the accuracy of model predictions.

Fluctuations of background signals are often the mechanisms for limiting the detectability of targets with particular systems, and may be even more important in a countermeasures environment. It is recommended that a dynamic sea background model be developed for use with the present target model.

### 5.3 Derivation of ship surface temperatures

#### 5.3.1 Equilibrium temperatures of solar heated surfaces

To obtain initial estimates of temperatures of the sunlit portions of ship surfaces, the plates may be considered as sufficiently thin or thermally conducting to allow both surfaces to be at the same temperature, and to have negligible thermal mass. The plates are irradiated by the sun on one side, and exchange heat by radiation and convection with the surroundings on both sides.

The thermal input powers per unit area of plate surface are:

(1) $F_s \cos w$ The solar irradiance on the plate where $F_s$ is the sea-level normal solar irradiance, and $w$ is the angle of the normal of the plate to the solar sight-line.

(2) $\varepsilon_p \sigma T_1^4$ The radiation absorbed from ambient at absolute temperature $T_1$ onto side 1 of the plate where $\varepsilon_p$ is the emissivity of the plate surface, and $\sigma$ is Stefan's Constant.

(3) $\varepsilon_p \sigma T_2^4$ As (2) but for side 2 of the plate.

The thermal output powers per unit area of plate surface are:

(4) $aF_s \cos w$ The solar radiation reflected from the surface, where $a$ is the plate surface reflectivity for the solar sea level spectrum.

(5) $\varepsilon_p \sigma T_s^4$ The radiation from the plate surface at temperature $T_s$ into ambient 1.

(6) $\varepsilon_p \sigma T_s^4$ As (5) but into ambient 2.

(7) $(h_1+\beta_1 V_1)(T_s-T_1)$ The convection from surface 1 of the plate into ambient 1 where $h_1$ and $\beta_1$ are free and forced convection coefficients and $V_1$ is the wind velocity.

(8) $(h_2+\beta_2 V_2)(T_s-T_2)$ The convection from surface 2 of the plate into ambient 2.

The thermal power equation for equilibrium is therefore:

$$F_s \cos w + \varepsilon_p \sigma T_2^4 + \varepsilon_p \sigma T_1^4 = aF_s \cos w + 2\varepsilon_p \sigma T_s^4 + (h_1+\beta_1 V_1)(T_s-T_1)$$

$$+ (h_2+\beta_2 V_2)(T_s-T_2)$$

This equation can be solved to provide the values of $T_s$ by providing known values of $F_s$, $w$, $\varepsilon_p$, $\sigma$, $a$, $T_1$, $T_2$, $V_1$ and $V_2$ and choosing appropriate values of $h_1$, $h_2$, $\beta_1$ and $\beta_2$, the values for the outer surface depending on windspeed and aspect. It is expected that attributing values of $V_1$ for net wind speed across the various faces of the ship will be difficult, owing to the degree of exposure to or shelter from the relative wind direction.

It should be noted that $T_1$ is an effective temperature for the hemisphere subtended by a surface. It can be obtained by measurement using a radiometer with sufficiently wide waveband to cover all significant energy inputs. Alternatively $T_1$ could be calculated from atmospheric data to include single scattering and radiation from the molecules of the atmosphere.

5.3.2 Derivation of non-equilibrium surface temperatures

Because the plates of the ship do have thermal mass, the equilibrium temperatures are only reached after some time of continuous irradiation under constant conditions. In general solar irradiation is not constant owing to changes of sun angle, cloud cover, and ship heading.

The equation of Section 5.3.1 can be modified to incorporate changes of Fs and $\omega$ and to include thermal time constants of plates based on their thickness, specific gravity and specific heat. If the plates are thin and of metal, thermal conductivity should be sufficiently high to keep both surfaces at very similar temperatures.

In the absence of solar irradiation the outer surfaces of the ship will reach equilibrium temperatures between the inside temperatures (which include those of funnels and engine rooms) and the outside ambients.

5.3.3 Development of temperature prediction

The model may be developed by programming the equation of Section 5.3.1 and choosing the appropriate heat transfer coefficients to provide equilibrium temperatures. A solar position model is already available to provide $\omega$ from latitude, longitude, zulu time, and ship geometry and heading.

Further development to derive non-equilibrium temperatures along the lines of reference 4, requires research on plate materials and thicknesses and ship internal temperatures. (For the Frigates with superstructure of ¼ inch aluminium the thermal capacity is 4.1 W h m$^{-2}$ °C$^{-1}$. The corresponding value for the steel hull is 10.4 or 8.65 depending on position.)

Such developments would allow prediction of ship signatures after planned voyages and could be valuable in special military circumstances.

5.4 Extension to other ships and military targets

It is intended that one of each of the major ship types in the Royal Australian Navy will be modelled when suitable plans become available.

Although the intention is to develop methods of reducing the vulnerability of RAN ships, it would also be reasonable to model foreign ships to investigate their vulnerability in the infrared wavebands.

The method can also be applied to generating infrared images of other military vehicles such as tanks.

## 6. CONCLUSIONS AND RECOMMENDATIONS

A digital model for generating the infrared images of ships has been developed. Shape data for four ships have been used with the model to produce images and arrays of irradiances suitable for inputs to a missile model.

An engine plume model is needed to complete the images in the 3 to 5 μm waveband. An improved representation of background radiances is required for simulation of specific situations. A detailed model of the thermal effects at the ship surfaces is necessary to extend the model so that surface temperatures are calculated from the thermal history.

## 7. ACKNOWLEDGEMENTS

The author thanks Mr R.J. Whatmough of Computing Services Group, ERL for assistance in operating the colourgraphics display equipment, and acknowledges the programming work of Mr J. Zervos of Infrared and Optical Countermeasures Group, ERL, and useful discussions with Dr S. Brunker also of this Group.

## NOTATION

| | |
|---|---|
| $A$ | area ($m^2$) |
| $A_1$, $A_2$ | rotation matrices |
| $B_\lambda$ | normalised spectral sensitivity at wavelength $\lambda$ |
| $C_1$ | first radiation constant ($W\ cm^2$) |
| $C_2$ | second radiation constant ($cm\ ^\circ K$) |
| $E_T$ | irradiance from background ($W\ cm^{-2}$) |
| $E_u$ | irradiance from upper hemisphere on area A (W) |
| $E_L$ | irradiance from lower hemisphere on area A (W) |
| $F_s$ | sea level normal solar irradiance ($W\ cm^{-2}$) |
| $H$ | radiant intensity ($W\ sr^{-1}$) |
| $J_{REF}$ | reflected intensity ($W\ sr^{-1}$) |
| $M_{R1}$ | missile position in reference system |
| $R$ | range (km) |
| $R_E$ | radius of Earth (km) |
| $R_1$ | axes subscript for reference system |
| $R_2$ | axes subscript for sight-line system |
| $T$ | temperature ($^\circ K$) |
| $T_{R1}$ | target position in reference system |
| $T_s$ | temperature of sea surface ($^\circ K$) |
| $V$ | velocity ($cm\ s^{-1}$) |
| $X$, $Y$, $Z$ | axes systems |
| $a$ | reflectivity |

| | |
|---|---|
| $dA_1$, $dA_2$ | elemental areas ($cm^2$) |
| $h$ | free convection coefficient ($W\ m^{-2}\ {}^{\circ}K^{-1}$) |
| $x$ | bow coordinate of ship element |
| $y$ | port coordinate of ship element |
| $z$ | height coordinate of ship element |
| $x_p$, $y_p$, $z_p$ | ship element coordinates in sight-line system |
| $Z$ | azimuth angle limit (°) |
| $\alpha$ | inclination to vertical (°) |
| $\beta$ | forced convection coefficient ($W\ m^{-3}\ {}^{\circ}K\ s$) |
| $\gamma$ | angle of reflection (°) |
| $\delta_R$ | declination of sight-line (°) |
| $\delta_H$ | declination of horizon (°) |
| $\delta_{RH}$ | angular separation of horizon and sight-line (°) |
| $\epsilon$ | emissivity |
| $\theta$ | Euler rotation (°) |
| $\lambda$ | wavelength (μm) |
| $\rho$ | azimuth angle (°) |
| $\sigma$ | Stefan's constant ($W\ m^{-2}\ {}^{\circ}K^{-4}$) |
| $\phi$ | elevation angle (°) |
| $\psi$ | Euler rotation (°) |
| $\omega$ | angle of plate normal to sight-line (°) |

## REFERENCES


| No. | Author | Title |
|---|---|---|
| 1 | Kneizys, F.X. et al | "Lowtran 6". AFGL Technical Report in Preparation |
| 2 | Scott, O.S. et al | "Ship Infrared Signature Reduction Experiments at Sea of a Water Cooling Method". ERL Technical Report ERL-0387-TR September 1986, Confidential |
| 3 | Oermann, R. | "Radiometry Using Thermal Imagers Part 1 - The Thermal Analysis Facility". ERL Technical Report ERL-0305-TR, March 1984, Unclassified |
| 4 | Burns, R.H. et al | "Description of the Ship Infrared/Electro Optical Scenarios (SIREOS) Computer Model, Report No 1". NSDC Report DTNDC-80/077 November 1986 |

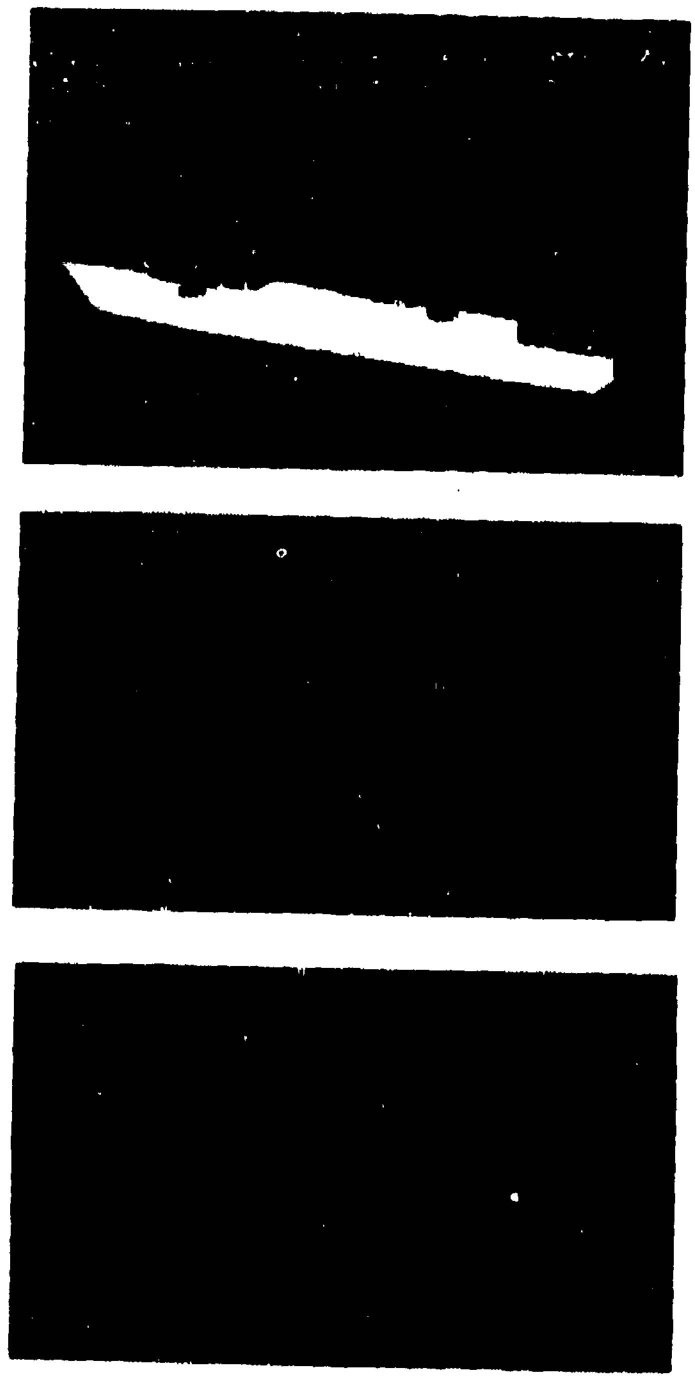

Figure 1. Samples of displayed output

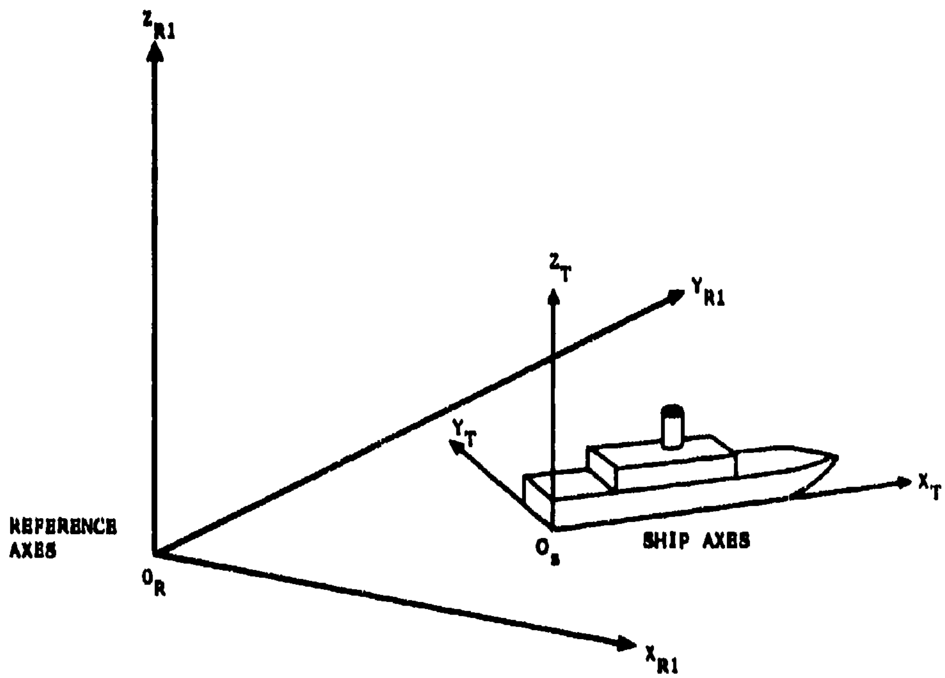


Figure 2. Ship and reference axes

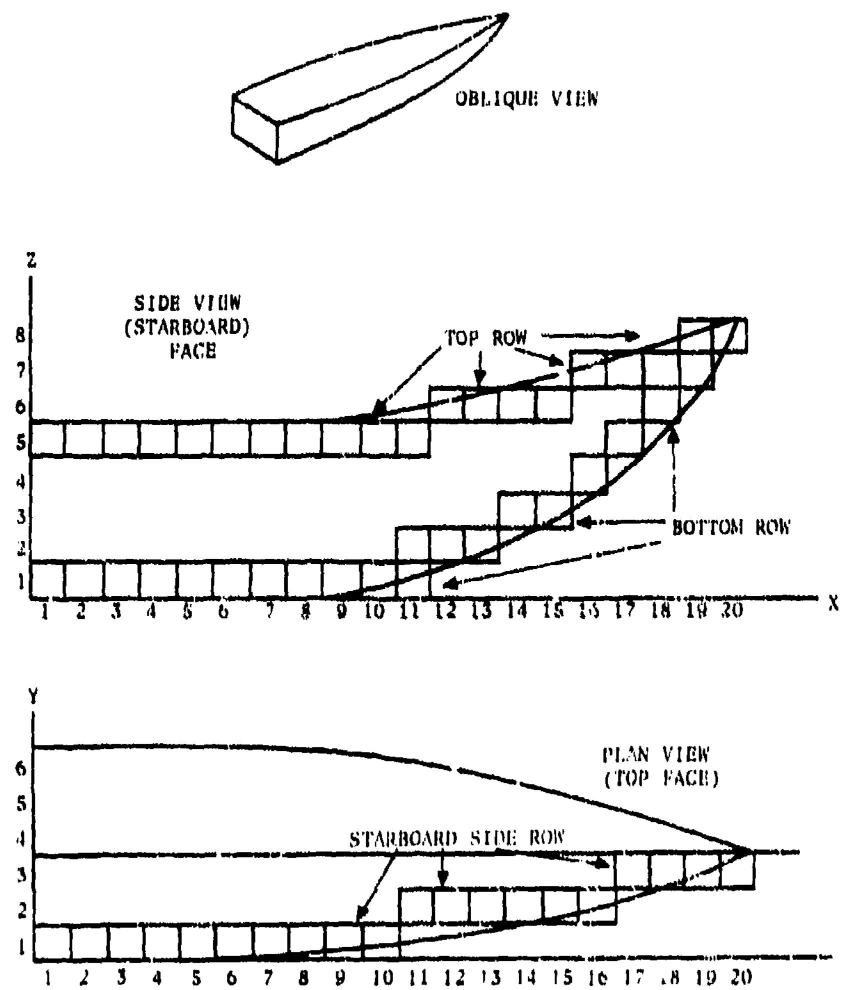


| | | | | | | | | | | | | | | | | | | | | |
|---|---|---|---|---|---|---|---|---|---|---|---|---|---|---|---|---|---|---|---|---|
| TOP | 05 | 05 | 05 | 05 | 05 | 05 | 05 | 03 | 05 | 05 | 05 | 06 | 06 | 06 | 06 | 07 | 07 | 07 | 08 | 08 |
| BOTTOM | 01 | 01 | 01 | 01 | 01 | 01 | 01 | 01 | 01 | 01 | 02 | 02 | 02 | 03 | 03 | 04 | 05 | 06 | 07 | 08 |
| SIDE | 01 | 01 | 01 | 01 | 01 | 01 | 01 | 01 | 01 | 01 | 02 | 02 | 02 | 02 | 02 | 02 | 03 | 03 | 03 | 03 |

Ship
"Centre" 10.5, 3.5, 3.5

Figure 3. Simple example of shape data

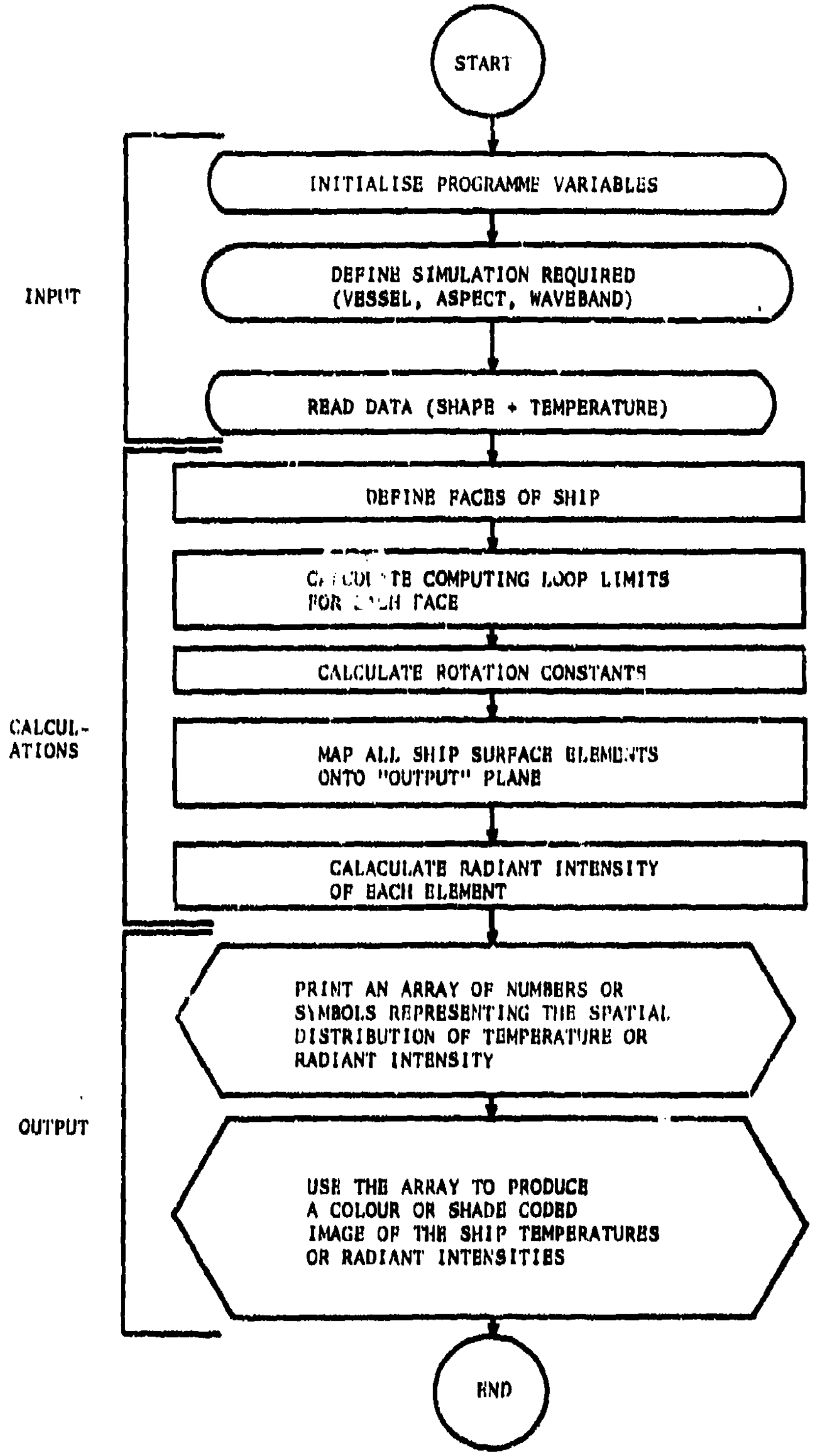


Figure 4. Flow diagram of model

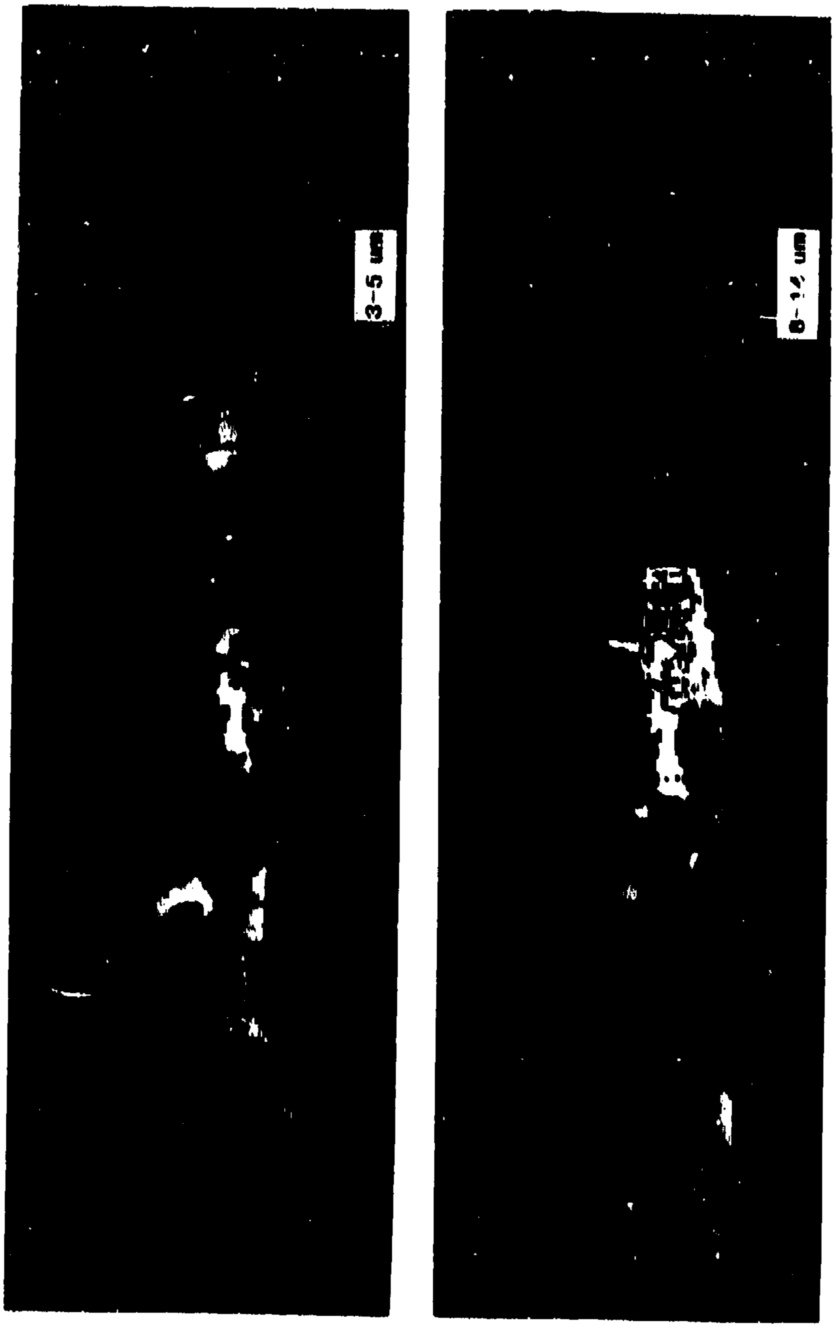


Figure 5. Measured images of HMAS Adelaide

THIS IS A BLANK PAGE

# APPENDIX I

## DERIVATION OF ROTATION EQUATION

### I.1 Sight-line axes (R2)

All points on the target are mapped onto a plane perpendicular to the sight line from the missile to the target (the output plane). Sight-line axes are $X_{R2}$ in the direction of the sight line, $Y_{R2}$ perpendicular to the upward vertical and to $X_{R2}$, and $Z_{R2}$ to complete the right-handed orthogonal set, ie:

$$X_{R2} = (T_{R1} - M_{R1})/|T_{R1} - M_{R1}|$$

$$Y_{R2} = (Z_{R1} \times X_{R2})/|Z_{R1} \times X_{R2}|$$

$$Z_{R2} = X_{R2} \times Y_{R2}$$

where $T_{R1}$ ($x_T$, $y_T$, $z_T$) and $M_{R1}$ ($x_M$, $y_M$, $z_M$) are the position vectors of the target and missile referred to the origin of reference axes $X_{R1}$, $Y_{R1}$, $Z_{R1}$ with $Z_{R1}$ chosen to be the upward vertical. The ship is assumed to be moving perpendicular to the $Z_{R1}$ axis with $z_T = 0$ and with no roll, pitch, or yaw.

### I.2 Rotation transform

Every point x, y, z referred to target axes ($X_T$ bow, $Y_T$ port, $Z_T$ vertically up) is expressed in coordinates ($x_p$, $y_p$, $z_p$) referred to sight-line axes, the Y-Z plane of which is the output plane so that screening of any point by another can be checked, and to provide the data for presentation of an image of the ship as seen from the missile.

Two Euler rotations $\psi$ and $\theta$ (figure I.1) are used to rotate the target axes (T) to align them with the reference axes (R1). $\psi$ is a rotation about $Z_T$ to bring $Y_T$ to $Y' = Y_{R2}$, perpendicular to $X_{R2}$, and $X_T$ to $X'$ ie:

$$\psi = \arctan\left(\frac{Y_{R2} \cdot X_T}{Y_{R2} \cdot Y_T}\right)$$

(and $\psi$ is the angle between the sight line and the ship bearing in the horizontal plane). $\theta$ is a rotation about the new $Y'$ axis to bring the new $X'$ axis into line with the $X_{R2}$ axis:

$$\theta = \arctan\left(\frac{Y_R \cdot Z_T}{X_{R2} \cdot (Y_{R2} \times Z_T)}\right)$$

(and $\theta$ is the angle between the sight line and the horizontal plane). The rotation transform is:

$$\begin{pmatrix} x_p \\ y_p \\ z_p \end{pmatrix} = A_2(\theta)A_1(\psi)\begin{pmatrix} x \\ y \\ z \end{pmatrix}$$

where

$$A_1 = \begin{bmatrix} \text{cosine} & \text{sine} & 0 \\ -\text{sine} & \text{cosine} & 0 \\ 0 & 0 & 1 \end{bmatrix} \text{ and } A_2 = \begin{bmatrix} \text{cosine} & 0 & -\text{sine} \\ 0 & 1 & 0 \\ \text{sine} & 0 & \text{cosine} \end{bmatrix}$$

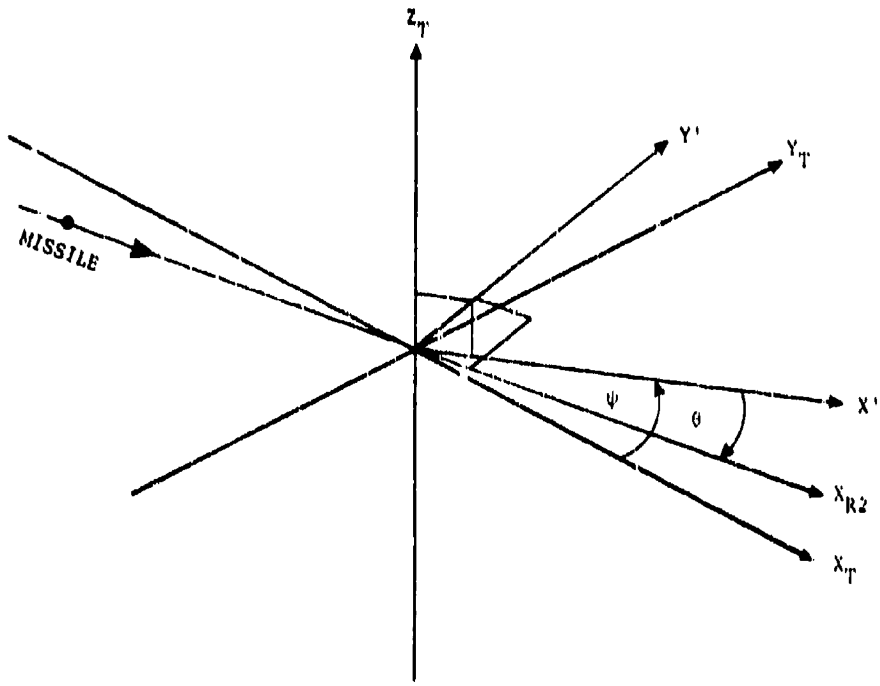


Figure 1.1 Rotation transform angles

## APPENDIX II

## REFLECTED "RADIANT" INTENSITY FROM AN INCLINED PLANE ELEMENT ORIGINATING FROM BACKGROUND

### II.1 Upper hemisphere

The background 'sky' radiance is assumed to be a function of elevation angle only. An element of sky background, $dA_2$, is represented by part of the area of the inside surface of a sphere of large radius $R_1$ between two caps, which is subtended by the plane element $dA_1$ inclined at $\alpha$ to the vertical (figure II.1).

If the element is at $\phi$ elevation and $\rho$ azimuth (figure II.1) the radiation falling onto $dA_1$ from $dA_2$ is:

$$\frac{dA_2\ dA_1\ (\cos\phi\ \cos\rho\ \cos\alpha\ -\ \sin\phi\ \sin\alpha)\ f(\phi)}{R_1^2}\ \mathrm{W}$$

where: $dA_2 = R_1^2 \cos\phi\ d\phi\ d\rho\ \mathrm{cm}^2$

and

$$f(\phi) = \frac{1}{\pi}\int_{\lambda_1}^{\lambda_2} \frac{C_1\ \lambda^{-5}\ B_\lambda\ d\lambda}{\exp C_2/\lambda T(\phi)}\ \mathrm{W\ sr^{-1}\ cm^{-2}}$$

The energy falling onto $dA_1$ from the whole horizontal section of the sphere is $dE_u$, given by:

$$dE_u = 2dA_1 \cos\phi\ f(\phi)\ d\phi \left[\cos\phi\ \cos\alpha \int_0^\Sigma \cos\rho\ d\rho\ -\ \sin\phi\ \sin\alpha \int_0^\Sigma d\rho\right] \mathrm{W}$$

and the energy falling onto $dA_1$ from the whole upper hemisphere is

$$E_u = 2dA_1 \left[ \cos\alpha \int_0^{\pi-a} \cos^2\phi \sin\Sigma \, f(\phi) \, d\phi \right.$$

$$\left. - \sin\alpha \int_0^{\pi-a} \cos\phi \sin\phi \, \Sigma \, f(\phi) \, d\phi \right] W$$

where $\Sigma = \arccos(\tan\phi \tan\alpha)$

II.2 Lower hemisphere

The apparent background sea radiance is assumed to be constant. An element of sea background $dA_2$ is represented by part of the area of the inside surface of a segment of a sphere of large radius $R_1$ (figure II.2).

If the element $dA_2$ is at $\phi$ declination and $\rho$ azimuth (figure II.2), the radiation falling onto $dA_1$ from $dA_2$ is:

$$\frac{dA_1(\cos\phi \cos\rho \cos\alpha - \sin\phi \cos\rho \sin\alpha) \, dA_2 F}{R_1^2}$$

where

$$dA_2 = R_1^2 \cos\rho \, d\phi \, d\rho \ \mathrm{cm}^2$$

and

$$F = \frac{1}{\pi} \int_{\lambda_1}^{\lambda_2} \frac{C_1 \lambda^{-5} B\lambda d\lambda}{\exp C_2/\lambda T_s} \ W \ sr^{-1}$$

where $T_s$ is the absolute temperature of the sea surface.

The energy falling onto $dA_1$ from the whole segment at $\phi$ is

$$dE_L = \left[ dA_1 \quad \cos\alpha \int_{-\frac{\pi}{2}}^{+\frac{\pi}{2}} \cos\phi \ \cos^2\rho \ d\phi d\rho - \sin\alpha \int_{-\frac{\pi}{2}}^{+\frac{\pi}{2}} \sin\phi \ \cos^2\rho \ d\phi d\rho \right] W$$

and from the whole lower hemisphere:

$$E_L = dA_1 \left[ \cos\alpha \int_{0}^{\frac{\pi}{2}+2} \int_{-\frac{\pi}{2}}^{+\frac{\pi}{2}} \cos\phi \ \cos^2\rho \ d\phi d\rho - \sin\alpha \int_{0}^{\frac{\pi}{2}+2} \int_{-\frac{\pi}{2}}^{+\frac{\pi}{2}} \sin\phi \ \cos^2\rho \ d\phi d\rho \right] W$$

## II.3 Reflected intensity

The total energy in the defined waveband falling onto $dA_1$ which originates from background is:

$$E_T = E_u + E_L \ W$$

A proportion of $E_T$, $(1 - \varepsilon)$ is reflected from the surface, and if this reflection is assumed to be lambertian (diffuse) the reflected intensity at any angle $\gamma$ to the normal of $dA_1$ is:

$$J_{REF \ \lambda_1 - \lambda_2} = \frac{dA_2 \cos\gamma(1-\varepsilon)E_T}{\pi} \ W \ sr^{-1}$$

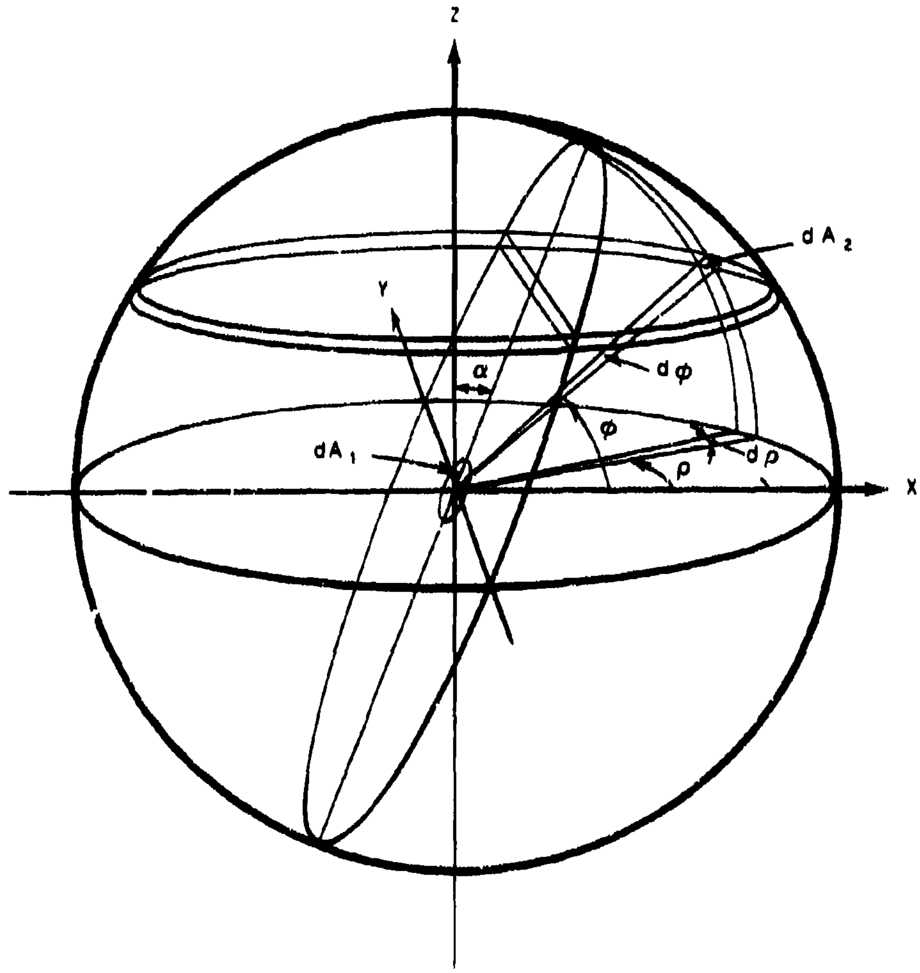


Figure II.1 Geometry of sky background irradiance calculation

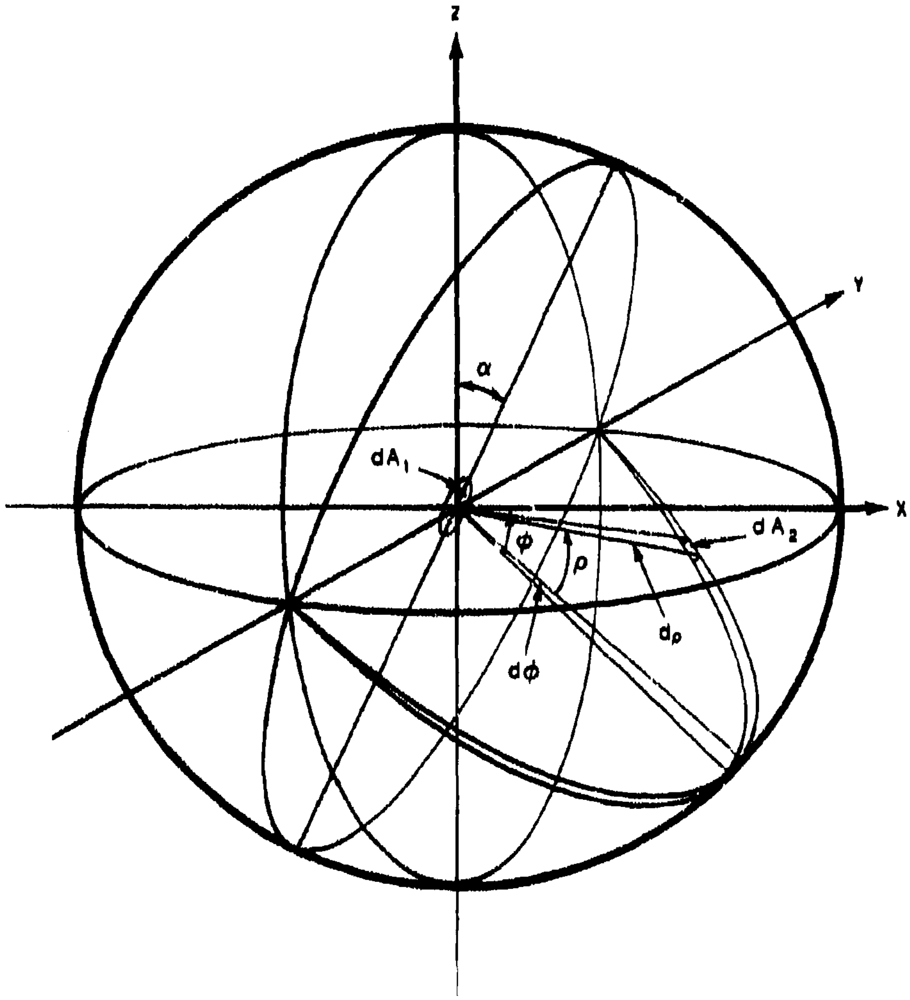


Figure II.2 Geometry of sea background irradiance calculation

## APPENDIX III

### DECLINATION OF SHIP REFERENCE POINT RELATIVE TO HORIZON

If the height of the missile and ship reference point above sea level are $z_M$ and $z_R$ respectively, and R is the distance between the two points, the declination $\delta_R$ of the reference point (from the horizontal) is, referring to figure III.1:

$$\delta_R = \sin^{-1}\left[\frac{R^2 + (R_E + z_M)^2 - (R_E + z_R)^2}{2R(z_M + R_E)}\right]$$

where $R_E$ is the radius of the Earth.

This reduces to:

$$\delta_R = \sin^{-1}\left(\frac{z_M - z_R}{R}\right)$$

when $z_R$, $z_M$ and R are small compared with $R_E$.

From figure III.2 the declination of the horizon (from the horizontal) is:

$$\delta_H = \cos^{-1}\left(\frac{R_E}{R_E + z_M}\right)$$

The horizon is therefore positioned at an angle ($\delta_{RH}$) in the image (or output) plane above the reference point given by:

$$\delta_{RH} = \delta_H - \delta_R$$

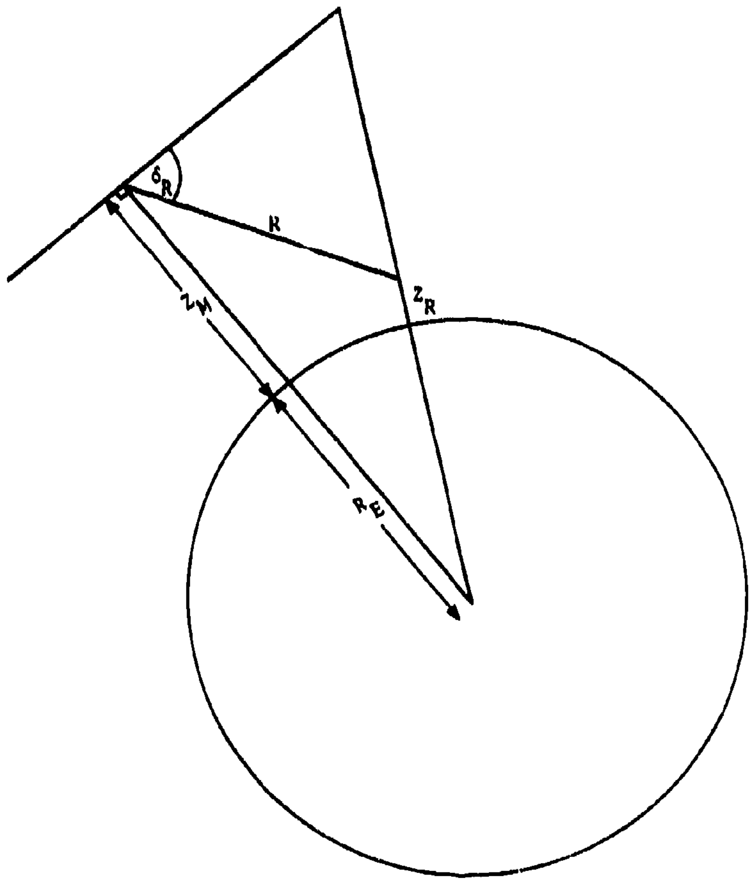


Figure III.1 Declination of reference point

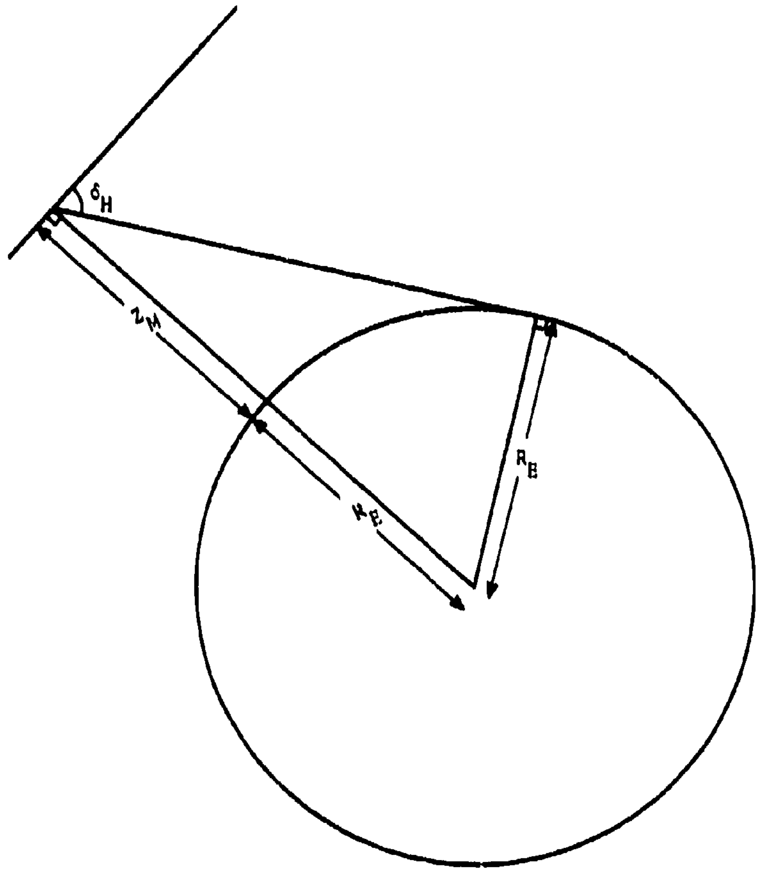


Figure III.2 Declination of horizon

DISTRIBUTION

| | Copy No. |
|---|---|
| DEPARTMENT OF DEFENCE | |
| Defence Science and Technology Organisation | |
| Chief Defence Scientist | 1 |
| Deputy Chief Defence Scientist | |
| Controller, External Relations, Projects and Analytical Studies | |
| Superintendent, Science Programs and Administration | |
| Counsellor, Defence Science, London | Cnt Sht Only |
| Counsellor, Defence Science, Washington | Cnt Sht Only |
| Superintendent, Analytical Studies | 2 |
| Electronics Research Laboratory | |
| Director, Electronics Research Laboratory | 3 |
| Superintendent, Electronic Warfare Division | 4 |
| Superintendent, Optoelectronics Division | 5 |
| Senior Principal Research Scientist, Electronic Warfare Division | 6 |
| Principal Officer, Infrared and Optical Countermeasures Group | 7 |
| Principal Officer, Information and Signal Processing Group | 8 |
| Principal Officer, Electronic Warfare Techniques Group | 9 |
| Principal Officer, Sensing and Propagation Group | 10 |
| Principal Officer, Systems Studies Group | 11 |
| Mr R.J. Whatmough, Computing Services Group | 12 |
| Mr J.G. Gardner, Infrared and Optical Countermeasures Group | 13 |
| Mr R.J. Oermann, Infrared and Optical Countermeasures Group | 14 |
| Mr J. Gravins, Infrared and Optical Countermeasures Group | 15 |
| Mr S. Brunker, Infrared and Optical Countermeasures Group | 16 |

| | |
|---|---|
| Weapons Systems Research Laboratory | |
| Director, Weapons Systems Research Laboratory | 17 |
| Principal Officer, Terminal Guidance Group | 18 |
| Principal Officer, System Modelling Group | 19 |
| Principal Officer, Systems Integration Group | 20 |
| Advanced Engineering Laboratory | |
| Director, Advanced Engineering Laboratory | 21 |
| Navy Office | |
| Navy Scientific Adviser | 22 |
| Director, Research Requirements | 23 - 24 |
| Army Office | |
| Scientific Adviser - Army | 25 |
| Joint Intelligence Organisation | 26 |
| Libraries and Information Services | |
| Librarian, Technical Reports Section, Defence Library, Campbell Park | 27 |
| Document Exchange Centre Defence Information Services Branch for: | |
| Microfiche copying | 28 |
| United Kingdom, Defence Research Information Centre | 29 - 30 |
| United States, Defense Technical Information Center | 31 - 42 |
| Canada, Director Scientific Information Services | 43 |
| New Zealand, Ministry of Defence | 44 |
| National Library of Australia | 45 |
| Main Library, Defence Research Centre Salisbury | 46 - 47 |
| Library, Aeronautical Research Laboratories | 48 |
| Library, Materials Research Laboratories | 49 |
| Library, Aircraft Research and Development Unit | 50 |
| Library, DSD | 51 |
| UNITED KINGDOM | |
| Royal Signals and Radar Establishment, Malvern (Attention: Dr M. Brown) | 52 |

| | |
|---|---|
| Admiralty Research Establishment, Portsdown<br>(Attention: Dr J. Heslop) | 53 |
| UNITED STATES OF AMERICA | |
| Naval Surface Weapons Centre, Silver Spring, Maryland<br>(Attention: Mr D. Wilson) | 54 |
| Author | 55 |
| Spares | 56 - 59 |

# DOCUMENT CONTROL DATA SHEET

Security classification of this page: UNCLASSIFIED

| 1 DOCUMENT NUMBERS | | 2 SECURITY CLASSIFICATION | |
|---|---|---|---|
| AR Number: | AR-004-885 | a. Complete Document: | Unclassified |
| Series Number: | ERL-0396-TR | b. Title in Isolation: | Unclassified |
| Other Numbers: | | c. Summary in Isolation: | Unclassified |

**3 TITLE**

A MATHEMATICAL MODEL FOR SIMULATING THE INFRARED IMAGES OF SHIPS

**4 PERSONAL AUTHOR(S):**

O.S. Scott

**5 DOCUMENT DATE:**

December 1986

**6**

6.1 TOTAL NUMBER OF PAGES 29

6.2 NUMBER OF REFERENCES: 4

**7 7.1 CORPORATE AUTHOR(S):**

Electronics Research Laboratory

7.2 DOCUMENT SERIES AND NUMBER

Electronics Research Laboratory 0396-TR

**8 REFERENCE NUMBERS**

a. Task: NAV 84/134

b. Sponsoring Agency:

**9 COST CODE:**

618056

**10 IMPRINT (Publishing organisation)**

Defence Research Centre Salisbury

**11 COMPUTER PROGRAM(S)** (Title(s) and language(s))

**12 RELEASE LIMITATIONS (of the document):**

Approved for Public Release

Security classification of this page: UNCLASSIFIED

Security classification of this page: UNCLASSIFIED

13 ANNOUNCEMENT LIMITATIONS (of the information on these pages):

No limitation

14 DESCRIPTORS:

a. EJC Thesaurus Terms

Mathematical models
Infrared images
Ships
Simulation
Infrared signatures
Infrared countermeasures

b. Non-Thesaurus Terms

15 COSATI CODES:

12010
17050

16 SUMMARY OR ABSTRACT:
(If this is security classified, the announcement of this report will be similarly classified)

This element-contribution model is programmed so that the distribution of infrared radiation from a ship target can be calculated for any aspect and any infrared waveband. The present application is to simulate the images formed by the guidance system of an imaging infrared antiship missile.

The input data needed are the surface temperatures and emmissivities and shapes of the main structures and the equivalent black body temperatures of the sky and sea surface. The shape of each ship is represented as a number of 'boxes' with each side and the top of each box represented by faces of elementary cubes. The positions and the centres of each face are calculated from the positions of three rows of elementary faces measured from plans for each box.

The output is an array of numbers representing the radiant intensity from the unscreened faces in the required direction and for the defined waveband. This array can be converted to a colour-coded image on a video display for testing and presentation purposes.

Security classification of this page: UNCLASSIFIED